Paper 242

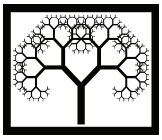

Proceedings of the Ninth International Conference
on Computational Structures Technology,
B.H.V. Topping and M. Papadrakakis, (Editors),
Civil-Comp Press, Stirlingshire, Scotland

An Efficient Computational Algorithm to Evaluate Fatigue Crack Growth under Variable Amplitude Loading from Strain-Life Data

J.T.P. Castro[1], M.A. Meggiolaro[1] and A.C.O. Miranda[2]
[1] Mechanical Engineering Department
[2] Civil Engineering Department
Pontifical Catholic University of Rio de Janeiro, Brazil

Abstract

Assuming that fatigue cracks grow by sequentially breaking small volume elements (VE) ahead of their tips, and modeling the cracks as sharp notches to remove their unrealistic singularity, the strain fields that surround them are obtained by fitting an HRR-like distribution to the finite strain at the notch root calculated by a suitable concentration rule. The damage caused by each load cycle, including the effects of residual stresses, are calculated at each VE using the hysteresis loops induced by the loading history. This approach is validated by comparing measured data for three alloys with predicted $\mathbf{da/dN \times \Delta K}$ curves, which are based only on $\boldsymbol{\varepsilon N}$, toughness and threshold properties, since the model does not need any fitting constant. This idea is extended to predict fatigue crack growth (FCG) under variable amplitude loading, equalizing the broken VE width to the region ahead of the crack tip that suffers damage beyond its critical value in each cycle.

Keywords: fatigue crack growth, critical damage, non-singular strain field, variable amplitude loading.

1 Introduction

Since the pioneer work of Majumdar and Morrow in 1974 [1], several models have been proposed to correlate fatigue crack initiation process, controlled by the strain range $\boldsymbol{\Delta\varepsilon}$, with fatigue crack growth (FCG) rates, controlled by the stress intensity range $\boldsymbol{\Delta K}$, assuming that the FCG process is associated with the sequential failure of small volume elements (VE) ahead of their tips. Some of this so-called critical damage models assume that the width of the VE in the crack propagation direction is the distance that the fatigue crack propagates on each cycle **da**. Others suppose that the FCG rate is given by a characteristic VE width divided by the number of cycles that the crack needs to cross it. However, most models assume that the crack has a zero radius singular tip, which implies that the VE adjacent to the crack tip suffers an in-

finite damage. This problem is usually avoided by introducing a fitting constant in the model, a trick that spoils their prediction capability.

But a recently proposed model [2], which requires no adjustable constant, recognizes that the actual elastic-plastic strain at the crack tip must be finite. It uses cyclic mechanical properties and a modified HRR distribution to describe the elastic-plastic strain field ahead of the crack tip. The crack is modeled as a sharp notch with a very small but finite tip radius, to remove its unrealistic singularity. Adapting an idea proposed by Creager and Paris [3], the origin of the HRR field is shifted from the crack tip to a point inside the crack, located by matching the HRR-like strain at the blunt crack tip with the strain predicted at that point by a suitable strain concentration rule. Or else, the strain range close to the crack tip is limited by the concentration rule, as explained below.

This model considers that the damage zone ahead of a fatigue crack tip is composed by (or dividable in) a sequence of tiny VE, which generally are under different strain ranges at any given instant, and which are sequentially broken as the crack propagates. In fact, the model assumes that FCG is ***caused*** by such sequential VE failures. Each one of these VE is submitted to elastic-plastic hysteresis loops whose range tends to increase as the crack tip approaches them. In each **j**-th load event, any **i**-th VE is damaged by the strain range $\Delta\varepsilon_i(r_i, \Delta K_j)$, which depends on its distance r_i from the crack tip, and on the stress intensity range ΔK_j at that event. The VE at the crack tip fractures when the damage it accumulated at each load cycle reaches a critical value, quantified by an appropriate damage accumulation rule, see Fig. 1.

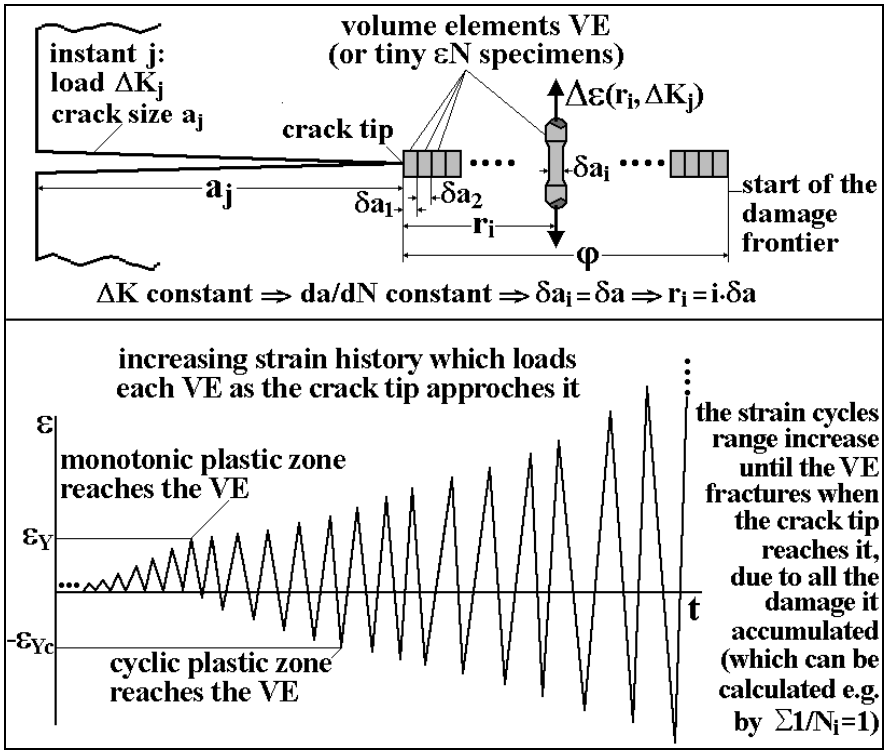

Figure 1: Schematics of the FCG assumed to be caused by the sequential fracture of small volume elements (or tiny εN specimens) at every load cycle, loaded by an increasing strain history as the crack tip approaches them.

The idea that FCG is caused by the sequential failure of VE ahead of the crack tip is then extended to deal with the variable amplitude loading (VAL) case. However, the modeling of FCG under VAL requires the recognition of load sequence effects which can severely affect fatigue lives and thus cannot be neglected in practice.

There are many mechanisms that can induce load sequence effects, retarding or accelerating the FCG after significant load amplitude variations [4-7]. Moreover, these mechanisms generally can act simultaneously in a way that can be competitive or symbiotic, with their relative importance in any problem depending on several factors such as: the crack and the piece sizes, dominant stress state at the crack tip, microstructure of the material, mean load, and environment. It is interesting to separate the several load interaction mechanisms by how they operate in relation to the crack tip. Thus, the various mechanisms are said to act ***behind***, ***at*** or ***ahead*** of the crack tip, and among them it is worth mentioning: fatigue crack closure (a mechanism that act ***behind*** the crack tip), which can be caused by plasticity, oxidation or roughness of the crack faces, or strain induced phase transformation, e.g.; crack tip blunting, kinking or bifurcation (mechanisms acting ***at*** or close to the crack tip); and residual stress and strain fields (whose influence is felt ***ahead*** of the crack tip).

Most models used to date to describe load sequence effects in FCG are still based on Elber's plasticity-induced crack closure, despite all its limitations. Indeed, there are several important problems that simply cannot be explained by the effective stress intensity range $\mathbf{\Delta K_{eff}}$ concept. For example, a strong objection against crack closure is based on convincing experimental evidence such as fatigue crack growth threshold values $\mathbf{\Delta K_{th}}$ that are higher in vacuum than in air [8]. Another very important problem that cannot be explained by the Elber mechanism is the crack delays or arrests after overloads under high $\mathbf{R = K_{min}/K_{max}}$ ratios, when the minimum value $\mathbf{K_{min}}$ of the applied stress-intensity range $\mathbf{\Delta K = K_{max} - K_{min}}$ always remains ***above*** $\mathbf{K_{op}}$, the (measured) load that opens the fatigue crack. In this case there is no closure, neither before nor after the overloads, see [9] for further details.

2 The Non-Singular Damage Model

Critical damage models are not new [1, 10-11], but they still need improvements. Most models assume singular stress and strain fields ahead of the crack tip, concentrating in this way all or most of the damage very next to the tip. Thus they need some adjustable constant to fit the FCG **da/dN** data, irreversibly compromising their ***prediction*** potential in this way. However, the supposed crack tip singularity is a characteristic of the mathematical models that postulate a zero radius tip, not of the real cracks, which always have a blunt tip when loaded. In other words, real cracks must have finite strains at their tip under load, or else they would be unstable. This argument by no means implies that singular models are useless in fatigue, it simply recognizes that such models cannot describe stresses and strains close to crack tip.

To avoid this problem, the actual finite strain range at the crack tip $\mathbf{\Delta\varepsilon_{tip}}$ can be estimated using the stress concentration factor $\mathbf{K_t}$ for the blunt crack [3] and an adequate strain concentration rule. Using this approach, the material ahead of the crack

tip is modeled as usual as continuous, isotropic and homogeneous. These classical hypotheses are in general only applicable to sizes or length scales larger than the parameter which characterizes the intrinsic non-homogeneity of the material's microstructure. But they work well in fatigue even when the crack increment is much smaller than that. Indeed, the crack growth rate **da/dN** is widely recognized as a phenomenon that is controlled by the stress intensity range $\Delta\mathbf{K}$ and peak $\mathbf{K_{max}}$, both homogeneous parameters.

It could be supposed that all fatigue damage occurs inside the region next to the crack tip, and use the number of cycles $\mathbf{N^*}$ associated with $\Delta\boldsymbol{\varepsilon_{tip}}$ (which can be obtained from Coffin-Manson's rule, e.g.) to calculate the FCG rate can as the length of this region divided by $\mathbf{N^*}$. But this modeling procedure has two shortcomings. First, neglecting the fatigue damage elsewhere, it concentrates all the damage in the very last $\mathbf{N^*}$ cycles, a non-conservative hypothesis. Second, to assume that fatigue crack increments are intermittent instead of induced by every load cycle, although valid in some cases of crazing in polymers, is certainly not true for most metallic structures, as evidenced by their striated crack surfaces.

To avoid these limitations, the model proposed here uses Schwalbe's modification [10] of the HRR field to describe the strain range distribution ahead of the crack tip. It removes the crack tip singularity by shifting the origin of the strain field from the crack tip to a point inside the crack, located by matching the tip strain with $\Delta\boldsymbol{\varepsilon_{tip}}$ predicted by a strain concentration rule, such as Neuber [12], Molsky and Glinka [13], or the linear rule [14]. Or else by maintaining the strain range field at and ahead of the crack tip upper-bounded by $\Delta\boldsymbol{\varepsilon_{tip}}$, assuming that such strain range remains limited by the value where the singular solution would predict strains greater than $\Delta\boldsymbol{\varepsilon_{tip}}$.

This approach recognizes that the strain range $\Delta\boldsymbol{\varepsilon}(\mathbf{r}, \Delta\mathbf{K})$ in all unbroken VE ahead of the crack tip changes, being able to cause damage in every fatigue load cycle as the crack tip approaches them, see Fig. 1. In this way, the strain range increases monotonically under constant amplitude load, as the distance of the VE to the crack tip decreases while the crack grows. Therefore, the VE closest to the tip breaks due to the accumulation of the damage induced by all previous load cycles, and not only by the damage induced in the very last load cycle. Thus, assuming that the constant FCG obtained under constant $\Delta\mathbf{K}$ is caused by the sequential failure of identical VE of width **da** aligned ahead of the crack tip, the rate **da/dN** is obtained by calculating the damage that any VE accumulates during its fatigue life.

This model is then extended to deal with the variable amplitude loading case. First, the VE that breaks in any given cycle can have variable width, which should be calculated by locating the point ahead of the crack tip where the accumulated damage reaches a specified value (e.g. 1.0 when using Miner's rule). Load sequence effects, such as overload-induced FCG retardation, are associated with residual mean load effects caused by elastic-plastic hysteresis loop shifts, which can be conveniently calculated using the numerical tools available in the **ViDa** software described elsewhere [7, 9], see [15] for details. Moreover, this model can recognize an opening load, and thus it can also separate the cyclic damage from the closure contributions to the crack growth process.

2.1 Constant Amplitude Loading

The idea under constant amplitude loading is to recognize that in every load cycle each i-th VE ahead of the crack tip suffers strain loops of increasing range $\Delta\varepsilon_i$ as the tip approaches it, and a damage increment that depends on the strain range in that cycle. Thus, the fatigue damage depends on r_i, the distance from the i-th VE to the tip, and on the load ΔK_j at that j-th load event (ΔK_j is obviously fixed when the load has constant amplitude). The fracture of the VE at the crack tip occurs because it accumulated its critical damage, e.g. by Miner when $\Sigma(1/N_j) = 1$, where N_j is the number of cycles that the piece would last if loaded solely by that **j**-th load event. Note that a VE of width **da** is broken at every load cycle when the crack is propagating at a constant rate **da/dN**.

If under constant ΔK (or ΔK_{eff}) the fatigue crack advances a fixed distance δa in every load cycle, and if, for simplicity, the damage outside the cyclic plastic zone zp_c is neglected, there are thus $zp_c/\delta a$ VE ahead of the crack tip at any instant. Since the plastic zone advances with the crack, each new load cycle breaks the VE adjacent to the crack tip, induces an increased strain range in all other unbroken VE, and adds a new element to the damage zone. Moreover, since the VE are considered as small εN specimens, they break when

$$\sum_{i=0}^{zp_c/\delta a} \frac{1}{N(zp_c - i\cdot\delta a)} = \sum_{r_i=0}^{zp_c} \frac{1}{N(r_i)} = 1 \tag{1}$$

where $N(r_i) = N(zp_c - i\cdot\delta a)$ is the fatigue life corresponding to the plastic strain range $\Delta\varepsilon_p(r_i)$ acting at a distance r_i from the crack tip, which can be calculated using the plastic part of Coffin-Manson's rule:

$$N(r_i) = \frac{1}{2}\left(\frac{\Delta\varepsilon_p(r_i)}{2\varepsilon_c}\right)^{1/c} \tag{2}$$

The strain range $\Delta\varepsilon_p(r_i)$ in its turn can be described by Schwalbe's [10] modification of the HRR field:

$$\Delta\varepsilon_p(r_i) = \frac{2S_{Yc}}{E}\cdot\left(\frac{zp_c}{r_i}\right)^{\frac{1}{1+h_c}} \tag{3}$$

where S_{Yc} is the cyclic yield strength, h_c is the Ramberg-Osgood cyclic hardening exponent, and zp_c is the cyclic plastic zone size in plane strain, which can be estimated using Poisson's coefficient ν through, e.g.,

$$zp_c = \frac{(1-2\nu)^2}{4\pi\cdot(1+h_c)}\cdot\left(\frac{\Delta K}{S_{Yc}}\right)^2 \Rightarrow \quad N(r_i) = \frac{1}{2}\left[\frac{S_{Yc}}{E\varepsilon_c}\cdot\left(\frac{zp_c}{r_i}\right)^{\frac{1}{1+h_c}}\right]^{1/c} \tag{4}$$

The HRR field describes the plastic strains ahead of an idealized crack tip, thus it is singular at $r = 0$. But an infinite strain is physically impossible (a fact that, once again, does not mean that singular crack models are useless, but only that the damage close to the crack tip is not predictable by them). To eliminate this unrealistic

strain singularity, the origin of the HRR coordinate system is shifted into the crack by a small distance **X**, adapting Creager and Paris idea [3]:

$$\Delta\varepsilon_p(r+X)=\frac{2S_{Yc}}{E}\cdot\left(\frac{zp_c}{r+X}\right)^{\frac{1}{1+h_c}} \tag{5}$$

Approximating the VE width **δa** by a differential **da** at a distance **dr** ahead of the crack tip and the Miner's summation by an integral, which is easier to deal with [2], the FCG rate can be calculated by:

$$\frac{da}{dN}=\int_0^{zp_c}\frac{dr}{N(r+X)} \tag{6}$$

To determine **X** and **N(r + X)**, two paths can be followed. The first uses Creager and Paris' elastic shift **X = ρ/2**, where **ρ** is the actual crack tip radius, which can be estimated by **ρ = CTOD/2**, thus

$$X=\frac{\rho}{2}=\frac{CTOD}{4}=\frac{K_{max}^2\cdot(1-2\nu)}{\pi\cdot E\cdot S_{Yc}}\cdot\sqrt{\frac{1}{2(1+h_c)}} \tag{7}$$

The second path is more reasonable. Instead of arbitrating the strain field origin offset, it determines **X** by first calculating the crack (linear elastic) stress concentration factor $\mathbf{K_t}$ [3]:

$$K_t=2\Delta K/(\Delta\sigma_n\cdot\sqrt{\pi\rho}) \tag{8}$$

For any given combination of **ΔK** and $\mathbf{K_{max}}$ or **R**-ratio, it is possible to calculate **ρ** and $\mathbf{K_t}$ from (7) and (8), and then the strain range $\Delta\varepsilon_{tip}$ at the crack tip using a suitable strain concentration rule. Assuming that the material stress-strain behavior is described by the parabolic Ramberg-Osgood model with cyclic strain hardening coefficient $\mathbf{H_c}$ and exponent $\mathbf{h_c}$, and with a negligible elastic range, the Linear, Neuber and Molsky and Glinka concentration rules give, respectively:

$$\Delta\varepsilon_{tip}=\frac{K_t\cdot\Delta\sigma_n}{E}=\frac{2\Delta K}{E\sqrt{\pi\cdot CTOD/2}} \tag{9}$$

$$\begin{cases}\Delta\sigma_{tip}\cdot\Delta\varepsilon_{tip}=\cdot\dfrac{(K_t\Delta\sigma_n)^2}{E}=\dfrac{8\Delta K^2}{E\cdot\pi\cdot CTOD}\\ \Delta\varepsilon_{tip}=2\left(\dfrac{\Delta\sigma_{tip}}{2H_c}\right)^{1/h_c}\end{cases} \tag{10}$$

$$\begin{cases}\dfrac{2\Delta K^2}{E\cdot\pi\cdot CTOD}=\dfrac{\Delta\sigma_{tip}^2}{4E}+\dfrac{\Delta\sigma_{tip}}{1+h_c}\cdot\left(\dfrac{\Delta\sigma_{tip}}{2H_c}\right)^{1/h_c}\\ \Delta\varepsilon_{tip}=2\left(\dfrac{\Delta\sigma_{tip}}{2H_c}\right)^{1/h_c}\end{cases} \tag{11}$$

After calculating $\Delta\varepsilon_{tip}$ at the crack tip using one of these rules, the shift **X** of the HRR origin is obtained by:

$$\Delta\varepsilon_{tip} = \frac{2S_{Yc}}{E}\cdot\left(\frac{zp_c}{X}\right)^{\frac{1}{1+h_c}} \Rightarrow X = zp_c\cdot\left(\frac{2S_{Yc}}{E\Delta\varepsilon_{tip}}\right)^{1+h_c} \tag{12}$$

The strain distribution at a distance **r** ahead of the crack tip, $\Delta\varepsilon_p(r + X)$, without the singularity problem at the crack tip, can now be readily obtained by:

$$\frac{da}{dN} = \int_0^{zp_c} 2\cdot\left(\frac{2\varepsilon_c}{\Delta\varepsilon_p(r+X)}\right)^{1/c} dr \tag{13}$$

This prediction was experimentally verified in two steels, SAE1020 and API 5L X-60, and in a 7075 T6 Al alloy, using (13) to obtain the constant of the quite interesting McEvily **da/dN** equation, which describes the **da/dN×ΔK** curves using only one adjustable parameter:

$$\frac{da}{dN} = A\left[\Delta K - \Delta K_{th}(R)\right]^2\left(\frac{K_c}{K_c - [\Delta K/(1-R)]}\right) \tag{14}$$

K_c and $\Delta K_{th}(R)$ are the material fracture toughness and crack propagation threshold measured at the load ratio **R**. To guarantee the consistence of this experimental verification, all material properties (K_c, $\Delta K_{th}(R)$, the **εN** and the **da/dN** data) were measured by testing proper specimens manufactured from the same stock of the 3 materials, following ASTM standards. API 5L X-60, SAE 1020 and Al 7075 T6 alloy **da/dN×ΔK** experimentally measured data are compared with this simple model predictions in Figs. 2-4. Both the shape and the magnitude of the data are quite reasonably reproduced by this critical damage model, with the Linear rule generating better ***predictions***, probably because the tests were made under predominantly plane strain conditions. Moreover, since this model does ***not*** use any adjustable constant, this performance is certainly no coincidence.

Despite this encouraging performance, some remarks are still required. First, the damage beyond zp_c was neglected to simplify the numerical calculations, but as it accumulates at all points ahead of the crack tip, it is wiser to choose the damage origin by numerically testing its influence on **da/dN**, or better by comparing the predictions with FCG tests, as done later on. Second, FE calculations [16] indicate that there is a region adjacent to the blunt crack tip with a strain gradient much lower than predicted by the HRR field. These problems can be avoided by shifting the origin away from the tip by x_2 and assuming the crack-tip strain range $\Delta\varepsilon_{tip}$ constant over the region I of length x_1+x_2 shown in Fig. 3, where x_1 can be obtained equating $\Delta\varepsilon_{tip}$ and the HRR-calculated strain range, and the crack-tip stress range $\Delta\sigma_{tip}$ from:

$$\Delta\sigma_{tip} = \Delta\sigma(r = x_1) = 2S_{Yc}\cdot\left(\frac{zp_c}{x_1}\right)^{\frac{h_c}{1+h_c}} = 2S_{Yc}\cdot\left(\frac{E\cdot\Delta\varepsilon_{tip}}{2S_{Yc}}\right)^{h_c} \tag{15}$$

Then, following Irwin's classical idea, the value of the shift x_2 is obtained by integrating the stress field $\sigma(r)$, enforcing equilibrium of the applied force:

$$\int_0^{\infty}\Delta\sigma(r)dr = \int_0^{x_1+x_2}\Delta\sigma_{tip}dr + \int_{x_1}^{\infty}\Delta\sigma(r)dr \Rightarrow \int_0^{x_1}\Delta\sigma(r)dr = \int_0^{x_1+x_2}\Delta\sigma_{tip}dr \tag{16}$$

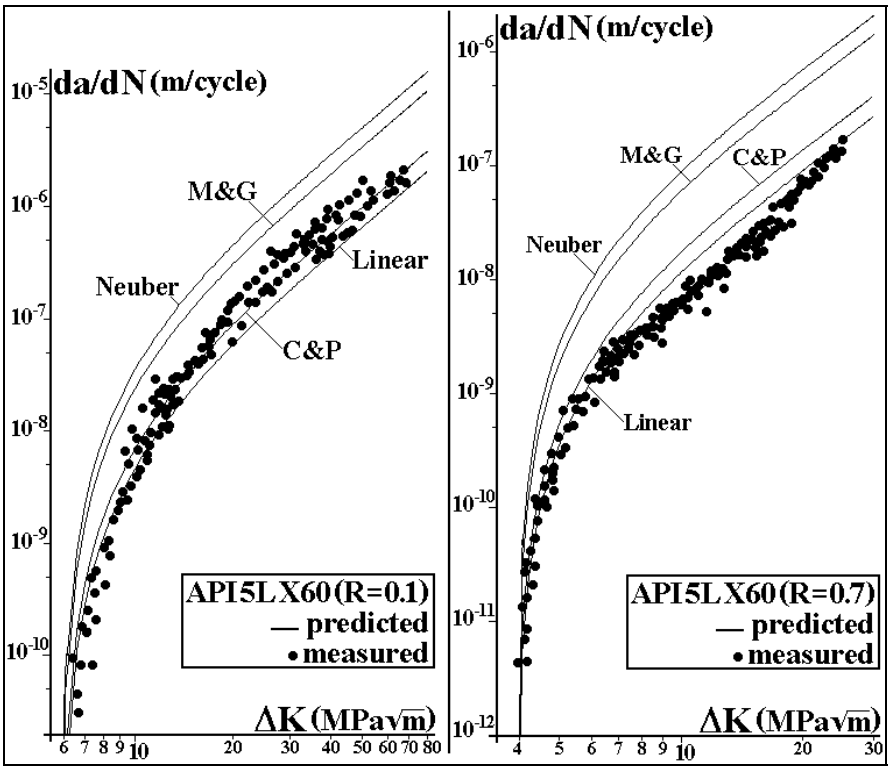

Figure 2: API-5L-X60 pipeline steel **da/dN×ΔK** FCG behavior measured at **R = 0.1** and at **R = 0.7**, and several curves ***predicted*** (not fitted) by the various strain concentration rules used in the critical damage model.

Since $x_1 < zp_c$, $\Delta\sigma(r)$ in the above integral can still be described by the HRR solution, resulting in

$$\int_0^{x_1} 2S_{Yc}\cdot\left(\frac{zp_c}{r}\right)^{\frac{h_c}{1+h_c}} dr = \Delta\sigma_{tip}\cdot x_1\cdot(1+h_c) = \Delta\sigma_{tip}\cdot(x_1+x_2) \Rightarrow x_2 = x_1\cdot h_c \qquad (17)$$

These simple procedures generate a probably more reasonable strain distribution model, schematized in Fig. 5:

$$\Delta\varepsilon(r) = \Delta\varepsilon_{tip}\ ,\ 0 \le r \le x_1 + x_2 \text{ (region I in Fig. 5)} \qquad (18)$$

$$\Delta\varepsilon(r) = \frac{2S_{Yc}}{E}\cdot\left(\frac{zp_c}{r-x_2}\right)^{\frac{1}{1+h_c}}\ ,\ x_1 + x_2 < r \le zp_c + x_2 \text{ (II, shifted HRR)} \qquad (19)$$

$$\Delta\varepsilon(r) \cong \frac{2S_{Yc}}{E}\cdot\sqrt{\frac{zp_c+x_2}{r}}\cdot(1+\nu\frac{r-zp_c}{zp-zp_c})\ ,\ zp_c + x_2 < r < zp \text{ (III, interpolation)} \qquad (20)$$

$$\Delta\varepsilon(r) = \frac{\Delta K\cdot(1+\nu)}{\kappa E\sqrt{2\pi\,(r-zp/2)}}\ ,\ r \ge zp \text{ (IV, shifted Irwin)} \qquad (21)$$

where $\kappa = 1$ for plane stress and $\kappa = 1/(1-2\nu)$ for plane strain, and where:

$$zp = \frac{1}{\pi\kappa^2}\cdot\left(\frac{K_{max}}{S_{Yc}}\right)^2 \text{ and } zp_c = \frac{1}{4\pi\kappa^2\cdot(1+h_c)}\cdot\left(\frac{\Delta K}{S_{Yc}}\right)^2 \qquad (22)$$

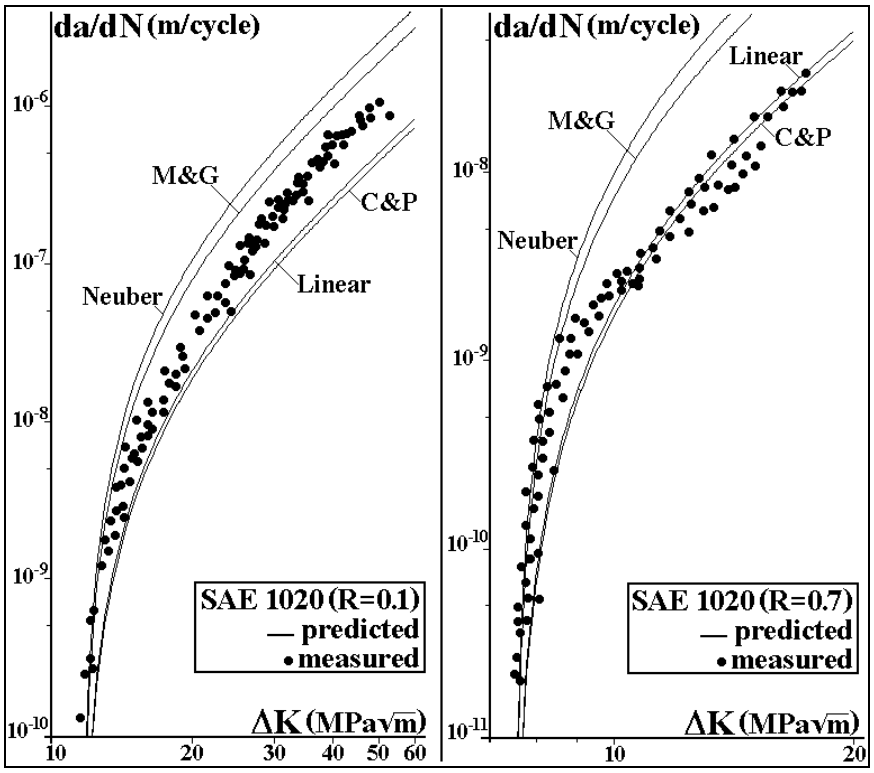

Figure 3: SAE 1020 steel **da/dN×ΔK** FCG behavior measured at **R = 0.1** and **0.7**, and several curves ***predicted*** (not fitted) by the various strain concentration rules.

2.2 Variable Amplitude Loading

Both constant (CA) and variable amplitude (VA) FCG can thus be calculated using equations (18-22), which consider all the damage ahead of the crack tip and provide a more realistic model of the FCG process. But (2), (5) and (13) must be modified to include elastic parameters σ_c and **b**, and to account for the mean load σ_m effects on the VE life using Morrow elastic, Morrow elastic-plastic or Smith-Topper-Watson equations. As the fatigue life **N** in these equations cannot be explicitly written as a function of the VE strain range and the mean load, it thus must be calculated numerically. However, such a programming task, despite introducing no major conceptual difficulty, is far from trivial.

The **da/dN×ΔK** curve predicted for CA loads could be used with a FCG load interaction model for treat VA problems. But the idea here is to *directly* quantify the fatigue damage induced by the VA load considering the crack growth as caused by the sequential fracture of ***variable*** width VE ahead of the crack tip. Since the Linear strain concentration rule generated better predictions above, it is the only one used here, and as load interaction effects can have a significant importance in FCG, they are modeled by using Morrow elastic equation to describe the VE fatigue life:

$$N(r+X)=\frac{1}{2}\left(\frac{\Delta\varepsilon_p(r+X)}{2\varepsilon_c}\left(1-\frac{\sigma_m}{\sigma_c}\right)^{-c/b}\right)^{1/c} \tag{23}$$

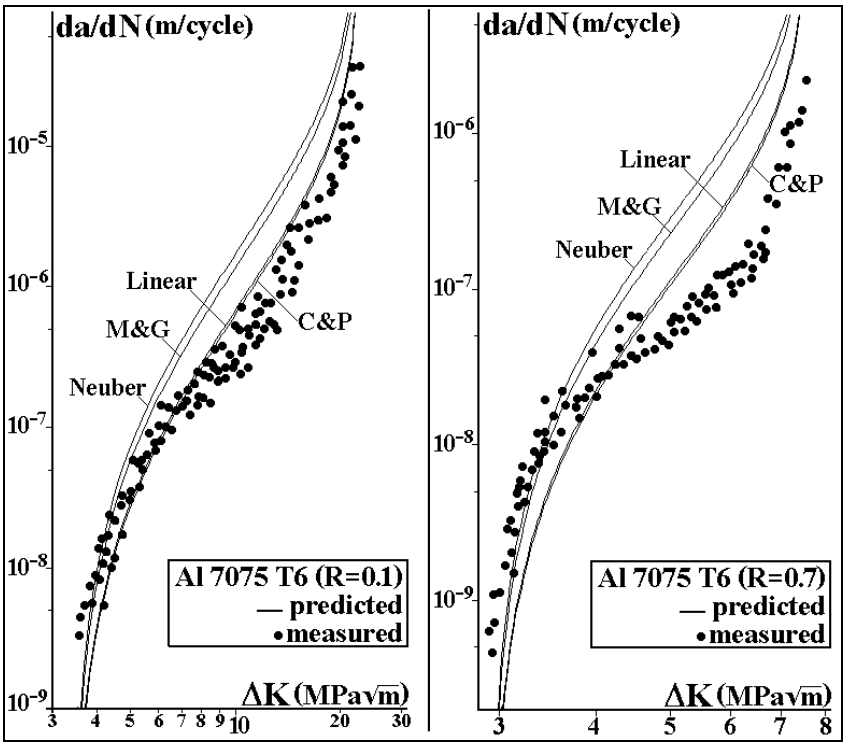

Figure 4: AL 7075 T6 **da/dN×ΔK** FCG behavior measured at **R = 0.1** and **R = 0.7**, and several curves ***predicted*** (not fitted) by the various strain concentration rules.

To account for mean load effects, a modified stress intensity range can be easily implemented for **R > 0** to filter the loading cycles that cause no damage by using:

$$\Delta K_{eff} = K_{max} - K_{PR} = \frac{\Delta K}{1-R} - K_{PR} \tag{24}$$

where K_{PR} is a propagation threshold that depends on the considered retardation mechanism, such as K_{op} or K_{max}^{*} from the Unified Approach [7]. The damage function for each cycle is then:

$$d_i(r + X_i) = \frac{n_i}{N_i(r + X_i)} \tag{25}$$

If the material ahead of the crack is supposed virgin, then its increment δa_1 caused by the first load event is the value $r = r_1$ that makes Equation (30) equal to one, therefore:

$$d_1(r_1 + X_1) = 1 \quad \Rightarrow \quad \delta a_1 = r_1 \tag{26}$$

In all subsequent events, the crack increments account for the damage accumulated by the previous loading, in the same way it was done for the constant loading case. But as the coordinate system moves with the crack, a coordinate transformation of the damage functions is necessary:

$$D_i = \sum_{j=1}^{i} d_j \left(r + \sum_{p=j}^{i-1} \delta a_p \right) \tag{27}$$

Since the distance $\mathbf{r} = \mathbf{r_i}$ where the accumulated damage equals one in the **i**-th event is a variable that depends on $\Delta\mathbf{K_i}$ (or $\Delta\mathbf{K_{eff_i}}$) and on the previous loading history, VE of different widths may be broken at the crack tip by this model. This idea is illustrated in Fig. 6.

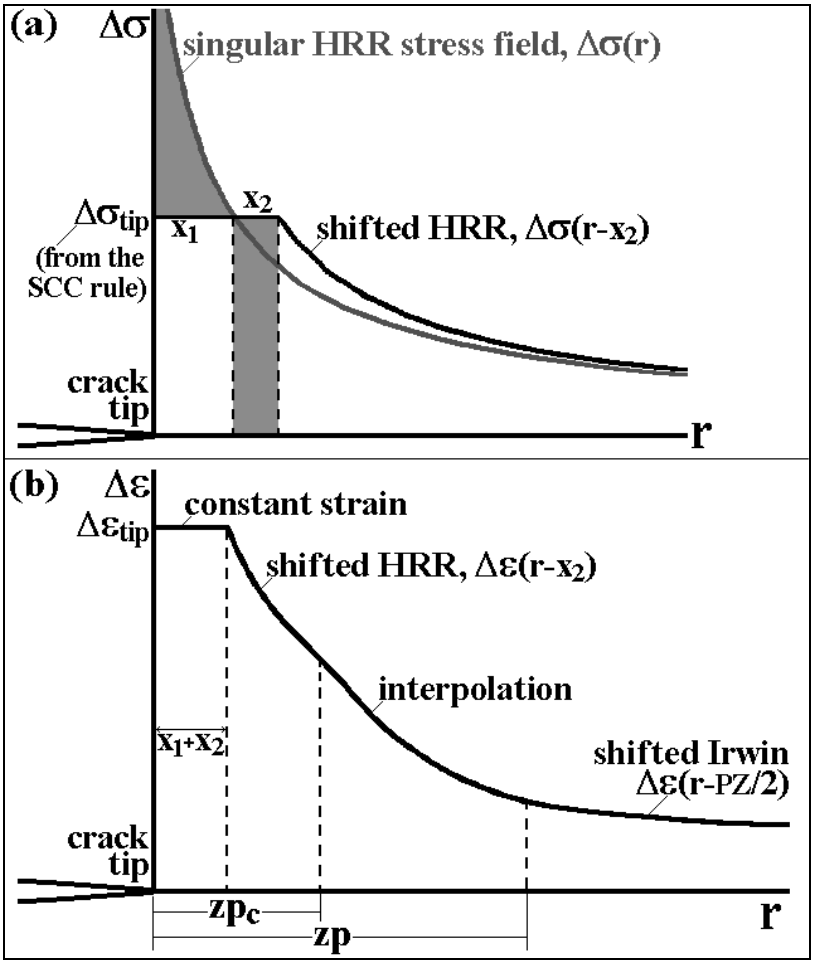

Figure 5: Proposed strain range distribution, divided into 4 regions to consider both the elastic and the plastic contributions to the damage ahead of the crack tip.

2.3 Simulation Algorithm for Variable Amplitude Loading

An algorithm is proposed to numerically implement the proposed methodology for variable amplitude loading. Instead of using variable width volume elements, which would be difficult to handle computationally since such widths are not known *a priori*, the algorithm assumes that all VE have constant width $\delta\mathbf{a}$. However, it allows the existence of a partially cracked VE at the crack tip, with residual ligament **rl**. The idea behind the calculations is to find at each cycle the number of fractured VE and the new value of **rl**, obtaining then the crack increment. The algorithm equations are described next.

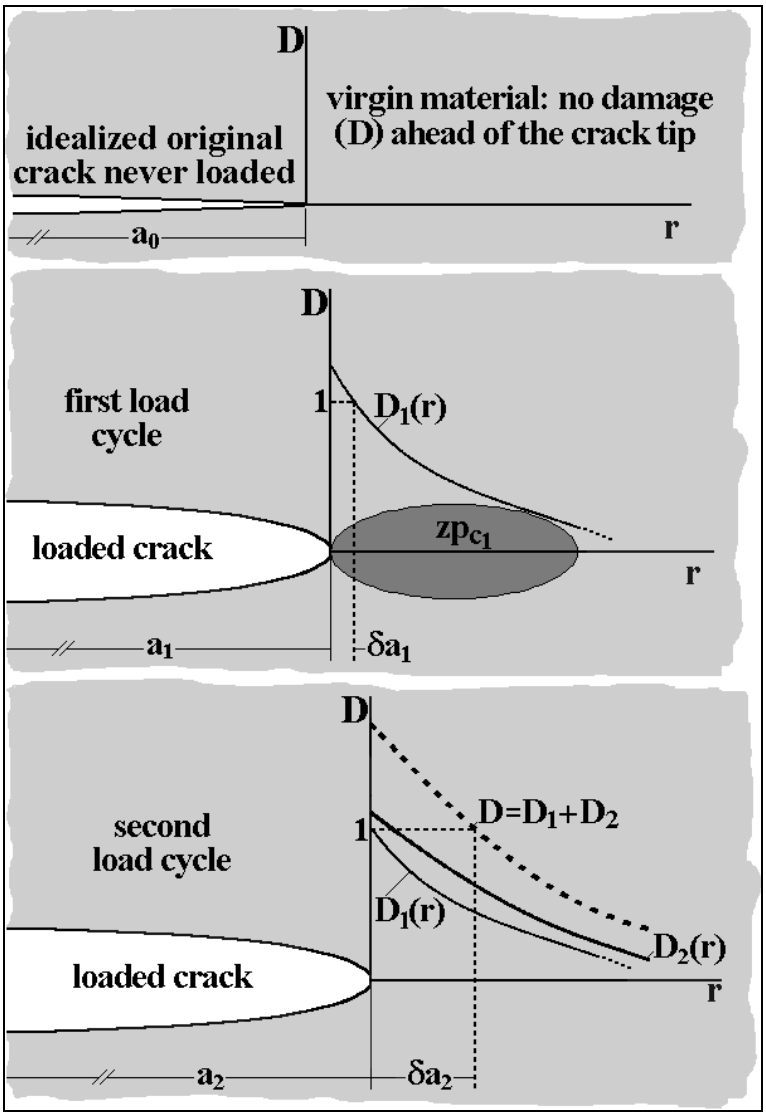

Figure 6: Schematics of the critical damage calculations, which under variable amplitude loading recognize variable crack increments by forcing the crack to grow over the region where **D = 1**.

First, upper bounds to the obtainable monotonic and cyclic yield zones are calculated. If the maximum values of $\mathbf{K_{max}}$ and $\mathbf{\Delta K}$ throughout the entire history are known, respectively $\mathbf{max(K_{max})}$ and $\mathbf{max(\Delta K)}$, then the upper bounds result in

$$\mathbf{zp_{max}} = \frac{\mathbf{1}}{\pi\kappa^2}\cdot\left(\frac{\mathbf{max(K_{max})}}{\mathbf{S_{Yc}}}\right)^2 \quad \text{and} \quad \mathbf{zp_{c,max}} = \frac{\mathbf{1}}{\mathbf{4\pi\kappa^2\cdot(1+h_c)}}\cdot\left(\frac{\mathbf{max(\Delta K)}}{\mathbf{S_{Yc}}}\right)^2 \qquad (28)$$

If these maximum values are not known *a priori*, then they can be conservatively replaced by the fracture strength $\mathbf{K_c}$ in the above equations.

The simulation resolution is set by the constant width $\mathbf{\delta a}$ of the VE, which is chosen in this work as 10^{-7}m. To reduce the memory requirements and speed up the algorithm, only a domain of length $\mathbf{\Delta a}$ ahead of the crack tip is considered, i.e., the

damage at the volume elements beyond this distance is neglected. Traditional critical damage models consider this domain **Δa** equal to the size of the current cyclic yield zone. However, this may lead to non-conservative errors because the plastic deformation between the monotonic and cyclic yield zones also contributes to significant accumulated damage. But in general it is not necessary to evaluate the damage at VE beyond the monotonic zone **zp**, where the accumulated damage would still be very close to zero.

In this work, two domain sizes **Δa** are considered, either $\mathbf{zp_{max}}$ or $\mathbf{zp_{c,max}}$. Note that these domains are already overestimated, since they use the upper bounds of **zp** or $\mathbf{zp_c}$, and not their values at each loading. This guarantees that the size of the calculation domain will be always larger than the monotonic or cyclic plastic zones, independently of the loading history.

For a resolution **δa** and domain length **Δa**, the accumulated damage needs to be calculated at the borders of an integer number $\mathbf{n = \Delta a/\delta a}$ of VE. This is accomplished by a set of **n** variables $\mathbf{D_1, D_2, \ldots, D_n}$, see Fig. 7. Note in this figure that the integer variable **k** denotes the index of the variable $\mathbf{D_k}$ associated with the damage at the next border of the VE where the crack tip is currently located. These **n** damage variables form a cyclic set, meaning that the variable $\mathbf{D_n}$ will be followed by $\mathbf{D_1}$, see Fig. 7.

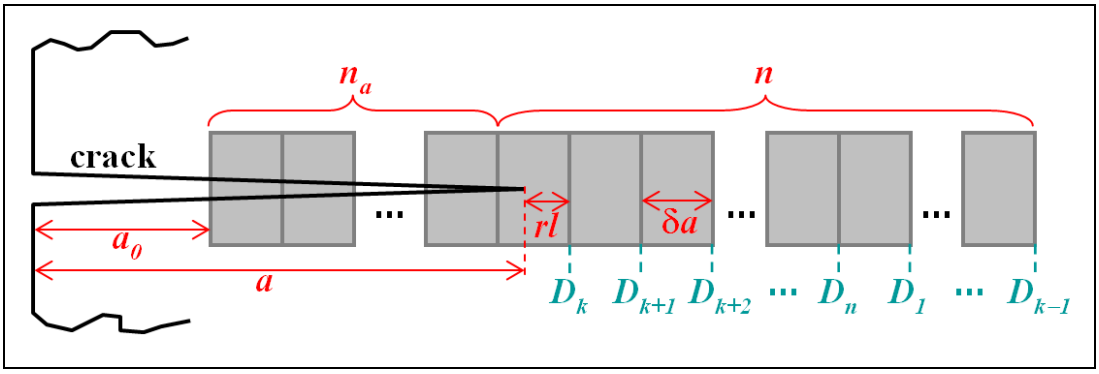

Figure 7: Volume elements before and ahead of the crack tip, showing the main length parameters and the locations for the calculation of the accumulated damages $\mathbf{D_1}$ through $\mathbf{D_n}$.

In this algorithm, the current crack size **a** is represented as a function of the initial crack length $\mathbf{a_0}$, an integer number $\mathbf{n_a}$ of already broken VE, and the residual ligament width **rl** in the partially cracked VE where the crack tip is currently located ($\mathbf{0 < rl \leq \delta a}$, see Fig. 7), by

$$\mathbf{a = a_0 + n_a \cdot \delta a + (\delta a - rl)} \tag{29}$$

In the beginning of the calculations, $\mathbf{rl = \delta a}$ and $\mathbf{n_a = 0}$, resulting in $\mathbf{a = a_0}$ as expected. In addition, all damage variables are initially set to zero, and $\mathbf{k = 1}$.

The applied loading is then counted using a sequential rain-flow algorithm [15] to preserve loading order. For each event, the alternate and mean nominal stresses are calculated, obtaining **ΔK**, $\mathbf{R = K_{min}/K_{max}}$, and the current plastic zone sizes **zp**

and $\mathbf{zp_c}$. If $\mathbf{\Delta K}$ is above the propagation threshold $\mathbf{\Delta K_{th}}$, which can indirectly include crack closure effects, then the damage at each VE is calculated.

The current **CTOD** and crack tip ρ are calculated from Eq.(7). The Eqs.(9-11) can then be used to obtain the crack tip stress and strain ranges, calculating the shift **X** of the HRR origin from Eq.(12).

Assuming that the damage caused by the current event can be neglected beyond the monotonic plastic zone, then at most the first $\mathbf{i_{max}}$ VE ahead of the crack tip need to be considered. Here, $\mathbf{i_{max}}$ is equal to **[int(zp/δa) + 2]**, where **int(x)** is the function that returns the largest integer smaller than or equal to **x**. The distance $\mathbf{r_i}$ between the crack tip and the $\mathbf{i^{th}}$ VE border beyond it, associated with $\mathbf{D_{k+i-1}}$, is

$$\mathbf{r_i = rl + (i - 1) \cdot \delta a} \tag{30}$$

The strain ranges $\mathbf{\Delta\varepsilon(r_i)}$ and associated damage are then calculated for $\mathbf{i = 1, \ldots, i_{max}}$. Such damage values at the VE borders are added to the accumulated $\mathbf{D_{k+i-1}}$. Then, the largest index $\mathbf{i = i_b}$ is found such that $\mathbf{D_{k+i_b-1} \geq 1}$ (or greater than any other parameter defined using Miner's rule). If $\mathbf{i_b}$ exists, then $\mathbf{i_b}$ VE are broken at the current event, and $\mathbf{i_b}$ is added to the total number $\mathbf{n_a}$ of broken elements. The new residual ligament **rl** in the first unbroken VE, to where the crack tip has advanced, is obtained from a linear interpolation between the accumulated damages at its borders:

$$\mathbf{rl = \delta a \cdot \frac{1 - D_{k+i_b}}{D_{k+i_b-1} - D_{k+i_b}}} \tag{31}$$

The $\mathbf{i_b}$ broken VE do not need anymore the variables $\mathbf{D_k}$ through $\mathbf{D_{k+i_b-1}}$, which are all reset to zero. Then, $\mathbf{i_b}$ new VE are created beyond the current domain border to keep the number of VE in the domain constant. The accumulated damage from these new VE will be stored in the just freed up variables $\mathbf{D_k}$ through $\mathbf{D_{k+i_b-1}}$. Note that $\mathbf{n_a}$ can eventually become larger than **n**, because of the new VE generated each time the crack advances. Finally, the index **k** is increased by $\mathbf{i_b}$, and the algorithm continues to evaluate the next event. It is easy to show that $\mathbf{k = (n_a \bmod n) + 1}$, where **(x mod y)** is equal to the remainder of the integer division between **x** and **y**. Note that if any index in the described algorithm results in a value **i** larger than **n**, then it is replaced by **(i mod n)**.

After all loadings have been sequentially considered in the calculations, the final crack size is evaluated using Eq.(29) and the final values of $\mathbf{n_a}$ and **rl**.

3 Experimental Results

FCG tests under VA loading were performed on an API-5L-X52 steel **50×10mm** C(T) specimens, which were pre-cracked under CA $\mathbf{\Delta K = 20MPa\sqrt{m}}$ until reaching crack sizes $\mathbf{a \cong 12.6mm}$. The cracks increments were redundantly measured within **20μm** accuracy by an optical traveling microscope and by the compliance method, bonding a strain gage on the back face of the specimens. The back face strain was always measured at maximum load, after assuring that the crack was completely opened. The basic monotonic and cyclic mechanical properties of this steel, meas-

ured in computer-controlled servo-hydraulic machines using standard testing procedures, are $\mathbf{E = 200{\cdot}10^3}$, $\mathbf{S_U = 527}$, $\mathbf{S_Y = 430}$, $\mathbf{S_{Yc} = 370}$, $\mathbf{H_c = 840}$, and $\boldsymbol{\sigma_c = 720}$ (all in MPa), $\mathbf{h_c = 0.132}$, $\boldsymbol{\varepsilon_c = 0.31}$, $\mathbf{b = -0.076}$ and $\mathbf{c = -0.53}$.

It is worth mentioning further details on the experimental procedures. About 50 εN specimens were tested under R-ratios varying from $\mathbf{R = -1}$ to $\mathbf{R = 0.8}$ (at least 2 specimens were tested at each strain range) to measure the mean load effect on the (fatigue crack initiation) εN curve, see Fig. 8. Morrow's elastic strain-life equation (23), which includes the mean stress effect only in Coffin-Manson's elastic term, best fit this experimental data.

The basic **da/dN** curve, measured using the same equipment, was well fitted by a modified Elber-type equation $\mathbf{da/dN(R = 0.1) = 2{\cdot}10^{-10}(\Delta K - 8)^{2.4}}$ (where **da/dN** in given in **m/cycle** and **ΔK** in **MPa√m**), using the crack propagation threshold $\mathbf{\Delta K_{th}(R = 0.1) = 8MPa\sqrt{m}}$ to replace $\mathbf{K_{op}}$.

FCG tests were then conducted under several VA histories. The history shown in Fig. 9 had 50,000 blocks containing 100 reversals each. Note the high mean stress levels, which were chosen to avoid crack closure effects (the crack was always opened during the loading). The load history was counted by the sequential rainflow method, using the **ViDa** software [15]. The damage calculation was made using a specially developed code following all the procedures discussed above.

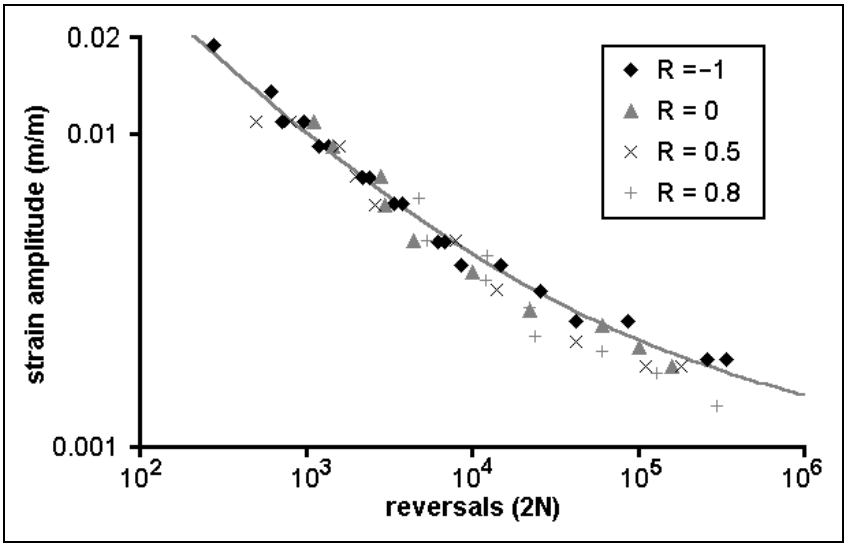

Figure 8: API 5L X52 steel strain-life data, and Morrow elastic model that best fitted this data.

The crack growth predictions based solely on **εN** parameters are again quite reasonable, see Fig. 10. The prediction assuming no damage outside the cyclic plastic zone $\mathbf{zp_c}$ underestimated the crack growth. However, when the small (but significant) damage in the material between the cyclic and monotonic plastic zone borders is also included in the calculations, an even better agreement is obtained. Note also that crack growth is slightly underestimated after $1.8{\cdot}10^6$ cycles, probably because these calculations neglected the (small) elastic damage and its mean stress effects.

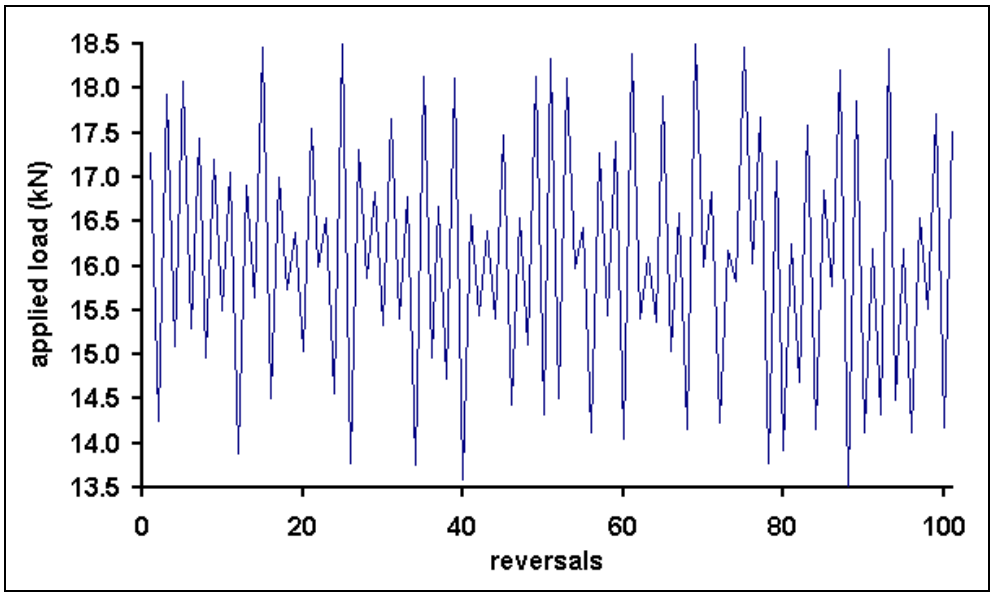

Figure 9: Variable amplitude load block applied to the API-5L-X52 steel. Note the high mean R-ratio.

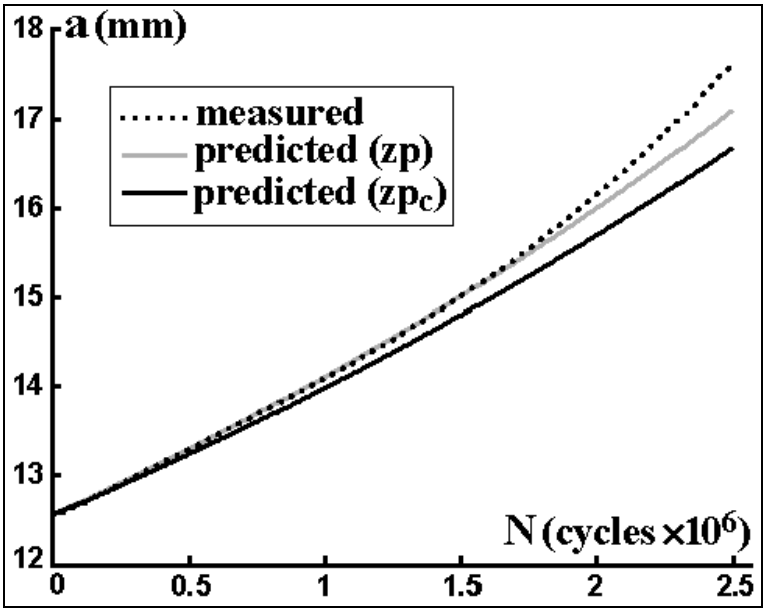

Figure 10: Comparison between the crack growth measurements and the εN-based predictions for the variable amplitude load presented in Fig. 6 (API-5L-X52 steel).

A similar VA FCG test was conducted on a specimen of AISI 1020 steel, with measured cyclic properties $\mathbf{E = 205GPa}$, $\mathbf{S_U = 491}$, $\mathbf{S_Y = 285}$, $\mathbf{S_{Yc} = 270}$, $\mathbf{H_c = 941}$ and $\mathbf{\sigma_c = 815MPa}$, $\mathbf{h_c = 0.18}$, $\mathbf{\varepsilon_c = 0.25}$, $\mathbf{b = -0.114}$, and $\mathbf{c = -0.54}$. The best FCG curve that could be fitted to this material was slight more complex than Elber's, namely $\mathbf{da/dN = 5 \cdot 10^{-10} \cdot (\Delta K - \Delta K_{th})^2 \cdot \{K_c/[K_c - \Delta K/(1 - R)]\}}$, where $\mathbf{\Delta K_{th} = 11.6}$ and $\mathbf{K_c = 277}$ ($\mathbf{\Delta K}$, $\mathbf{\Delta K_{th}}$ and $\mathbf{K_c}$ in $\mathbf{MPa\sqrt{m}}$ and $\mathbf{da/dN}$ in $\mathbf{m/cycle}$).

The VA load history is this case was a series of blocks containing 101 peaks and valleys, as shown in Fig. 11. Fig. 12 compares the prediction with the measured

data. This prediction was again quite reasonable. Therefore, one can claim that these tests indicate that the ideas behind the proposed critical damage model make sense and deserve to be better explored.

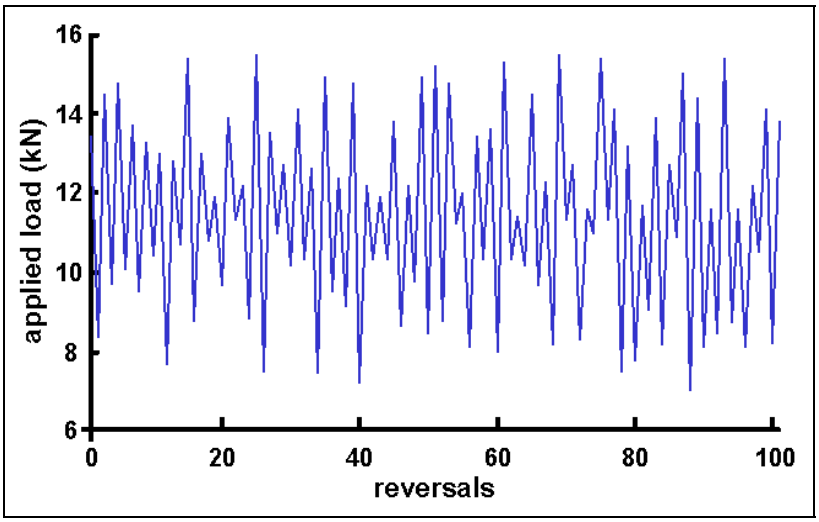

Figure 11: VA load block applied to the SAE 1020 steel C(T). Again a high mean R-ratio was used in this test, to avoid the interference of possible significant closure effects which could mask the model performance.

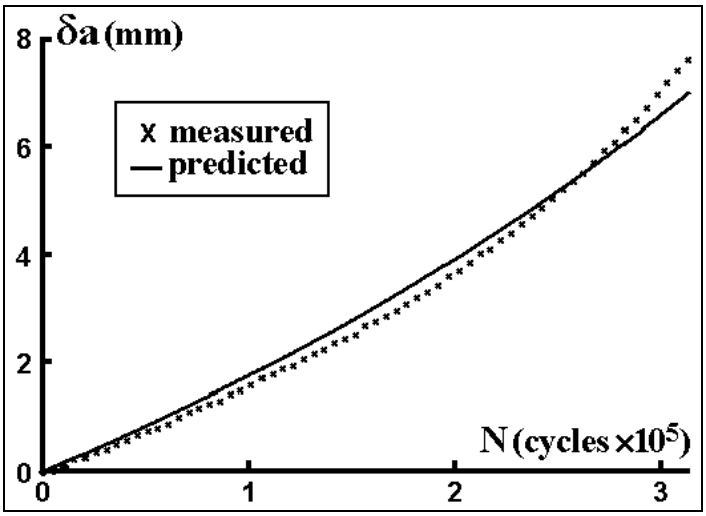

Figure 12: Comparison between the crack growth measurements and the εN-based predictions for the variable amplitude load presented in Fig.11 (SAE 1020 steel).

4 Conclusions

Several mechanisms can cause load sequence effects on fatigue crack growth, and they may act *before*, *at* or *after* the crack tip. Plasticity-induced crack closure is the most popular of them, but it cannot explain sequence effects in various important problems. A damage accumulation model ahead of the crack tip based on εN cyclic properties, which can explain those effects in the absence of closure, was proposed for predicting fatigue crack propagation under variable amplitude loading. The

model treats the crack as a sharp notch with a small but finite radius to avoid singularity problems, and calculates damage accumulation explicitly at each load cycle. Experimental results show a good agreement between measured crack growth both under constant and variable amplitude loading and the predictions based purely on εN data.

References

[1] S. Majumdar, J. Morrow, "Correlation Between Fatigue Crack Propagation and Low Cycle Fatigue Properties", ASTM STP 559, 159-182, 1974.

[2] J.A.R. Durán, J.T.P. Castro, J.C. Payão Filho, "Fatigue Crack Propagation Prediction by Cyclic Plasticity Damage Accumulation Models", FFEMS 26, 137-150, 2003.

[3] M. Creager, P.C. Paris, "Elastic Field Equations for Blunt Cracks with Reference to Stress Corrosion Cracking", Int. J. Fracture Mechanics 3, 247-252, 1967.

[4] S. Suresh, *Fatigue of Materials*, 2nd ed., Cambridge, 1998.

[5] M. Skorupa, "Load Interaction Effects During Fatigue Crack Growth under Variable Amplitude Loading - a Literature Review - Part I: Empirical Trends", FFEMS 21, 987-1106, 1998.

[6] M. Skorupa, "Load Interaction Effects During Fatigue Crack Growth under Variable Amplitude Loading - a Literature Review - Part II: Qualitative Interpretation", FFEMS 22, 905-926, 1999.

[7] J.T.P. Castro, M.A. Meggiolaro, A.C.O. Miranda, "Singular and Non-Singular Approaches for Predicting Fatigue Crack Growth Behavior", Int. J. Fatigue 27, 1366-1388, 2005.

[8] A.K. Vasudevan, K. Sadananda, R.L. Holtz, "Analysis of Vacuum Fatigue Crack Growth Results and its Implications", Int. J. Fatigue 27, 1519-1529, 2005.

[9] M.A. Meggiolaro, J.T.P. Castro, "On the Dominant Role of Crack Closure on Fatigue Crack Growth Modeling", Int. J. Fatigue 25, 843-854, 2003.

[10] K.H. Schwalbe, "Comparison of Several Fatigue Crack Propagation Laws with Experimental Results", Eng. Fracture Mechanics 6, 325-341, 1974.

[11] G. Glinka, "A Notch Stress-Strain Analysis Approach to Fatigue Crack Growth", Eng. Fracture Mechanics 21, 245-261, 1985.

[12] H. Neuber, "Theory of Stress Concentration for Shear-Strained Prismatical Bodies with an Arbitrary Non-Linear Stress-Strain Law", J. Applied Mechanics 28, 544-551, 1961.

[13] K. Molsky, G. Glinka, "A Method of Elastic-Plastic and Strain Calculation at a Notch Root", Materials Science and Engineering 50, 93-100, 1981.

[14] R. Stephens, A. Fatemi, R.R. Stephens, H.O. Fuchs, *Metal Fatigue in Engineering*, Interscience, 2000.

[15] www.tecgraf.puc-rio.br/vida, last accessed in April 1st 2008.

[16] V.Z. Parton, E.M. Morozov, *Elastic-Plastic Fracture Mechanics*, Mir Publishers, 1978.